

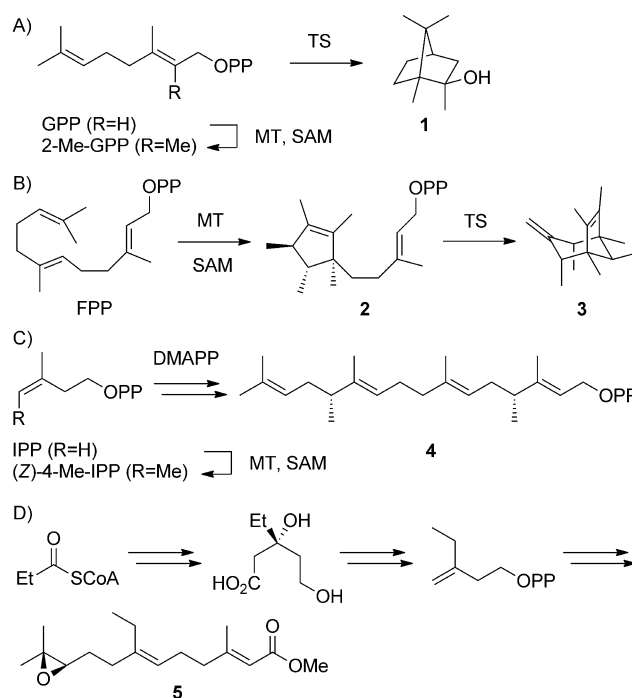
Terpenoids

Enzymatic Synthesis of Methylated Terpene Analogues Using the Plasticity of Bacterial Terpene Synthases

Anwei Hou, Lukas Lauterbach, and Jeroen S. Dickschat*^[a]

Abstract: Methylated analogues of isopentenyl diphosphate were synthesised and enzymatically incorporated into methylated terpenes. A detailed stereochemical analysis of the obtained products is presented. The methylated terpene precursors were also used in conjunction with various isotopic labellings to gain insights into the mechanisms of their enzymatic formation.

During the past decade the genome sequences of many bacteria and fungi became available, which allowed for the discovery and characterisation of various terpene synthases (TSs).^[1–7] Canonical TSs catalyse the conversion of isoprenoid diphosphates with the general formula (C_{5n}H_{8n+1})OPP including dimethylallyl (DMAPP, *n* = 1), geranyl (GPP, *n* = 2), farnesyl (FPP, *n* = 3), geranylgeranyl (GGPP, *n* = 4) and geranylgeranyl diphosphate (GGPP, *n* = 5) into terpenes. For the larger precursors (*n* > 1) the products are usually (poly)cyclic and contain multiple stereogenic centres. The TS-catalysed transformations proceed through substrate ionisation by abstraction of diphosphate or by protonation, followed by a cationic cascade including cyclisation reactions, hydride or proton migrations and skeletal rearrangements. The cascade is terminated by deprotonation to yield a terpene hydrocarbon (C_{5n}H_{8n}) or by the addition of water resulting in a terpene alcohol (C_{5n}H_{8n+2}O). Deviations from these general molecular formulae may point to non-canonical TSs that can catalyse the cyclisation of methylated terpene precursors (Scheme 1), exemplified by 2-methylisoborneol (1) that is formed by a methyltransferase (MT) through S-adenosyl-L-methionine (SAM) dependent methylation to 2-Me-GPP and cyclisation by a TS.^[8] For sodorifen (3) a MT catalyses a methylation-induced cyclisation to presodorifen diphosphate (2), followed by a second TS-dependent cyclisation.^[9] The recently investigated meroterpenoid longestin incorporates (4*R*,12*R*)-4,12-dimethyl-GGPP (4) that is generated by methylation of isopentenyl diphosphate (IPP) to (*Z*)-4-methyl-IPP, fol-



Scheme 1. Biosynthesis of the homoterpenes A) 2-methylisoborneol (1), B) sodorifen (3), C) (4*R*,12*R*)-4,12-dimethyl-GGPP (4), D) juvenile hormone II (5).

lowed by a programmed skipped incorporation into the isoprenoid diphosphate chain.^[10] Based on the uptake of radioactivity from [1–¹⁴C]propionate into *Manduca sexta* juvenile hormone II (5) a biosynthetic hypothesis by the passage of propionyl-CoA substituting for acetyl-CoA through the mevalonate pathway was proposed.^[11] In addition to such natural enzyme systems for the biosynthesis of homoterpenes, several canonical TSs exhibit a remarkable plasticity that allows the conversion of non-natural substrate analogues with additional Me groups or heteroatoms.^[12] This strategy can give a rapid and potentially enantioselective access towards methylated or functionalised terpene analogues, but previous work depended on the chemical synthesis of the oligoprenyl diphosphate analogues. Here we report on the stereoselective synthesis of homologated IPP derivatives, the enzymatic incorporation into methylated GPP and FPP analogues, and their TS-catalysed conversion into non-natural homoterpenes.

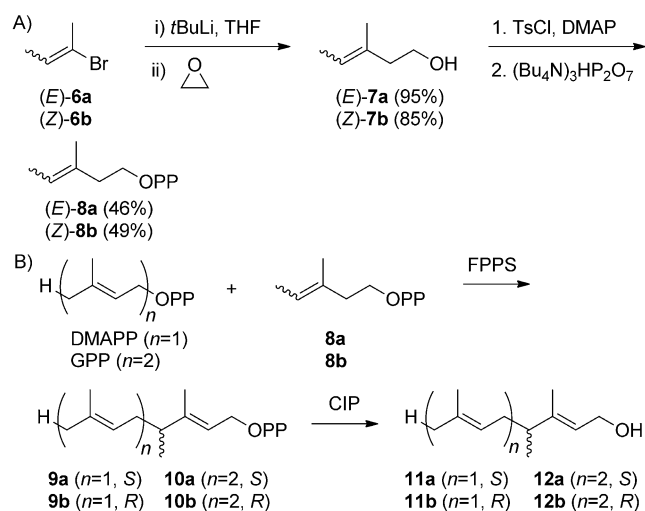
For the enzymatic synthesis of homoterpenes, (*E*)-4-methyl-IPP (8a) was stereoselectively synthesised from (*E*)-2-bromobut-2-ene (6a) by halogen–metal exchange with *t*BuLi and ad-

[a] Dr. A. Hou, L. Lauterbach, Prof. Dr. J. S. Dickschat
Kekulé-Institute of Organic Chemistry and Biochemistry
University of Bonn, Gerhard-Domagk-Strasse 1, 53121 Bonn (Germany)
E-mail: dickschat@uni-bonn.de

Supporting information and the ORCID identification number(s) for the author(s) of this article can be found under:
<https://doi.org/10.1002/chem.201905827>.

© 2020 The Authors. Published by Wiley-VCH Verlag GmbH & Co. KGaA. This is an open access article under the terms of the Creative Commons Attribution License, which permits use, distribution and reproduction in any medium, provided the original work is properly cited.

dition to oxirane to yield (*E*)-3-methylpent-3-en-1-ol (**7a**) (Scheme 2A). Conversion into the corresponding tosylate and nucleophilic substitution with $(\text{Bu}_4\text{N})_3\text{HP}_2\text{O}_7$ gave **8a**. Its stereoisomer (*Z*)-4-methyl-IPP (**8b**) was prepared via the same route



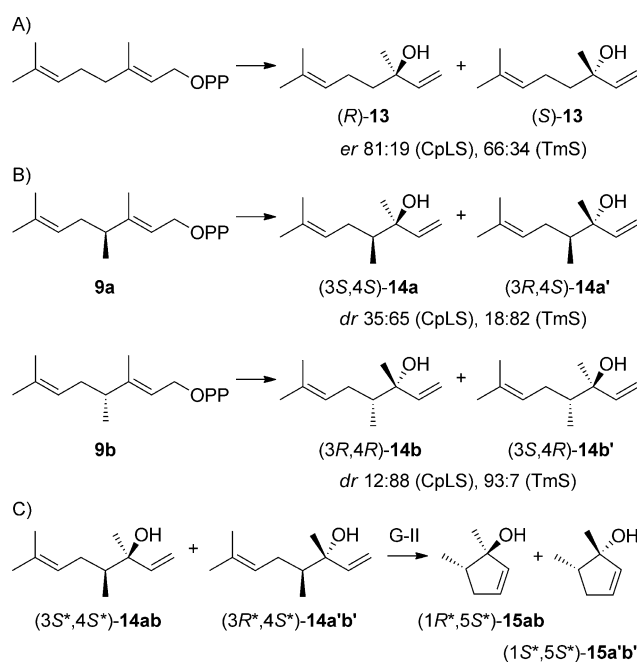
Scheme 2. Preparation of both enantiomers of 4-methyl-GPP (**9ab**) and 4-methyl-FPP (**10ab**). A) Chemical synthesis of (*E*)- and (*Z*)-4-methyl-IPP (**8ab**). B) Enzymatic coupling of DMAPP and GPP with **8ab** by FPPS.

starting from *Z* configured **6b**. Subsequently, DMAPP was elongated with **8a** and **8b** using the FPP synthase (FPPS) from *Streptomyces coelicolor* A3(2),^[13] followed by dephosphorylation with calf intestinal phosphatase (CIP). GC/MS analysis of the products suggested that with both substrates **8a** and **8b** mainly only one extension step to 4-methyl-GPP (**9**) was catalysed, whereas only very small amounts of double extension products were observed (Figure S1, Supporting Information). A preparative-scale incubation of DMAPP and **8a** (100 mg each) with FPPS followed by treatment with CIP allowed to isolate the main product that was identified by NMR spectroscopy (Table S1, Figures S2–S8) as 4-methylgeraniol (**11**). GC analysis using a chiral stationary phase revealed that the products **11** from **8a** and **8b** were enantiomers and were obtained in high enantiomeric purity (Figure S9). The elongation of GPP with **8a** and **8b** using FPPS also resulted in the two enantiomers of 4-methyl-FPP (**10**) with high enantiomeric purity, as demonstrated by dephosphorylation with CIP followed by GC/MS and enantioselective GC analysis (Figures S10 and S11). A preparative-scale reaction with **8a** and product isolation for structure elucidation by NMR (Table S2, Figures S12–S18) confirmed the structure of 4-methylfarnesol (**12**). Its optical rotation $[\alpha]_D^{20} = -6.0$ (CH_2Cl_2 , c 0.25) allowed to assign the absolute configuration of (*S*)-4-methylfarnesol (**12a**) for the product from **8a** by comparison to literature data for the same enantiomer ($[\alpha]_D = -10.7$, hexane),^[14] and consequently (*R*)-**12b** was obtained from **8b**. Based on the same sign for the optical rotation $[\alpha]_D^{20} = -5.5$ (CH_2Cl_2 , c 0.2) of **11a** formed from **8a**, and on the same GC elution order on a chiral stationary phase, analogous absolute configurations were assigned for (*S*)-**11a** and (*R*)-**11b**.

These findings are in agreement with the classical experiments regarding FPP biosynthesis that demonstrated *Si* face attack at C4 of IPP (because of a change in priority orders this corresponds to the 4*Re* face of **8a** and the 4*Si* face of **8b**).^[15]

In subsequent experiments bacterial terpene synthases were investigated for their potential to convert the methylated GPP and FPP analogues into methylated terpenes. For this purpose, a newly identified linalool synthase from *Chryseobacterium polytrichastri* DSM 26899 (CpLS, accession number WP 073293738) and the known T-muurolol synthase from *Roseiflexus castenholzii* DSM 13941 (TmS)^[16] were selected, because these enzymes showed a particularly effective conversion of their native substrates. While CpLS naturally accepts only GPP, but no FPP or GGPP, TmS shows most efficient conversion of FPP and also accepts GPP, but no GGPP. The main product obtained from GPP with purified CpLS (Figure S19, Supporting Information) was identified by GC/MS as linalool (**13**), besides minor amounts of geraniol and a few trace compounds (Figure S20). Compound **13** was obtained as a mixture of (*R*)- and (*S*)-linalool (81:19, 60% *ee*, Scheme 3A), as determined by chiral GC in comparison to authentic (*R*)-**13** (Figure S21). TmS converted GPP into a mixture of geraniol, (*R*)- and (*S*)-**13** (66:34, 33% *ee*), β -myrcene and a few minor compounds (Figures S20 and S21). CpLS and TmS were used in this study to obtain the poorly described 4-methylalools^[17] and to solve the difficult problem of their configurations.

The incubation of DMAPP and **8a** with FPPS and CpLS gave the two stereoisomers (3*S*,4*S*)-**14a** and (3*R*,4*S*)-**14a'** (*dr* 35:65), while the same reaction with **8b** yielded (3*R*,4*R*)-**14b** and (3*S*,4*R*)-**14b'** (*dr* 12:88) (Scheme 3B). Their configurations at C4 were inferred from the stereostructures of **9a** and **9b**, but it



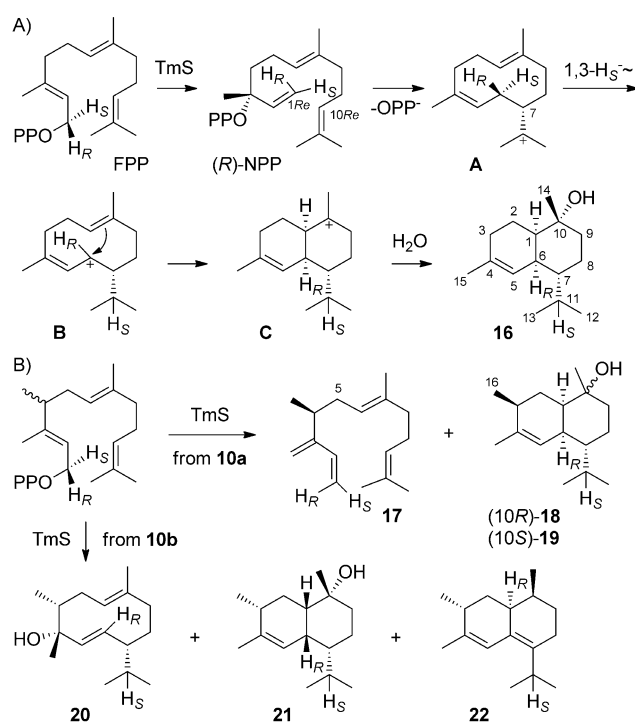
Scheme 3. Enzyme reactions with CpLS and TmS. Conversion of A) GPP into **13**, B) enzymatically prepared **9a** and **9b** into diastereomeric mixtures of **14**, and C) cyclisation of **14** with Grubbs II (G-II) catalyst.

could not be assigned at this stage which stereoisomer is major and which one is minor, because for the acyclic compounds it was not possible to determine the relative configuration at C3 by NOESY. For full structure elucidation the racemic mixture of all four stereoisomers of **14** was synthesised (Scheme S1, Supporting Information) and separated by chiral GC (Figure S22). This stereoisomeric mixture was then converted into the corresponding stereoisomers of **15** using the Grubbs II catalyst, followed by isolation of (1*R**,5*S**)-**15ab** and (1*S**,5*S**)-**15a'b'** by column chromatography (Scheme 3C), for which the relative configurations were solved by NMR spectroscopy (Tables S3 and S4, Figures S23–S36). The stereoisomeric mixture of **14** was separated by chiral HPLC, giving access to two pure stereoisomers of **14** that were identical to the minor enzyme product from **8a** with 4*S* and the major enzyme product from **8b** with 4*R* configuration, whereas the remaining two stereoisomers coeluted (Figure S37). NMR spectroscopy of the pure stereoisomers confirmed that they were diastereoisomers (Tables S5 and S6, Figures S38–S51). The Grubbs II cyclisation of (4*S*)-**14** yielded a product with the same retention time as one of the enantiomers of (1*R**,5*S**)-**15ab** on a chiral GC phase (Figure S52), establishing the full structure of (1*R*,5*S*)-**15** for this material and, conclusively, of (3*S*,4*S*)-**14** for its precursor, the minor enzyme product from **8a**. Thus, the major product is (3*R*,4*S*)-**14**. Similarly, (4*R*)-**14** was converted into a product with the same retention time as one of the enantiomers of (1*S**,5*S**)-**15a'b'**, thus identified as (1*R*,5*R*)-**15**. In conclusion, its precursor (3*S*,4*R*)-**14** is the major and (3*R*,4*R*)-**14** is the minor enzyme product from **8b**.

With **9b**, a high diastereoselectivity is observed for CpLS, even higher than its enantioselectivity with GPP, with attack of water at C3 preferentially from the substrates' *Re* faces at C3 in both cases, whereas the selectivity with **9a** is poor with attack of water mainly from the *Si* face. With TmS, **9a** was converted into (3*R*,4*S*)-**14a'** and (3*S*,4*S*)-**14a**, whereas from **9b** the products (3*R*,4*R*)-**14b** and (3*S*,4*R*)-**14b'** were obtained (Figure S22, Supporting Information). For this enzyme the attack of water at C3 of **9a** and **9b** proceeds with good to high diastereoselectivity mainly at the *Si* face, whereas for GPP *Re* face attack is preferred. These data suggest that the conformations of **9a** and **9b** in the active sites of CpLS and TmS in comparison to GPP are strongly influenced by the additional 4-Me group.

TmS converts FPP into T-muurolool (**16**) through a cascade with isomerisation to NPP, followed by cyclisation to **A**, a 1,3-hydride shift to **B**, cyclisation to **C** and attack of water (Scheme 4A). The installation of the stereocentre at C7 in **A** is explained by FPP isomerisation through *syn*-allylic transposition to (*R*)-NPP and *anti*-*S_N2'* attack with 1*Re*,10*Re* cyclisation, with a defined stereochemical course for the enantiotopic C1 hydrogens of FPP. As a consequence, the 1-*pro-S* hydrogen of FPP selectively migrates into the *iPr* group of **B**, as demonstrated experimentally by enantioselective deuteration of FPP.^[18]

GPP in conjunction with **8a** or **8b** was efficiently converted by FPPS and TmS, however, the observed product selectivity of TmS was much lower than with FPP and in both cases complex mixtures of sesquiterpenes were formed (Figure S53, Sup-



Scheme 4. Enzymatic conversions with TmS. A) Cyclisation mechanism from FPP to **16**, B) products obtained from **10a** and **10b** with TmS. Carbon numberings for **18–22** as for **16**, the additional Me group is numbered C16.

porting Information). From substrate **8a**, (5)-4-methyl-(*E*)- β -farnesene (**17**), (3*S*)-3-methyl-T-muurolool (**18**) and its epimer (3*S*)-3-methyl-10-*epi*-T-muurolool (**19**), formed by attack of water from the opposite face at C10 of a cation **C** analogue, were isolated (Scheme 4B), whereas the conversion of **8b** yielded (3*R*,4*R*,7*R*)-3-methyl-4-hydroxygermacra-1(10),5-diene (**20**), (3*R*)-3-methyl-1,6-*diepi*-T-muurolool (**21**) and (1*S*,3*R*,10*S*)-3-methylzorenarene (**22**) (NMR data: Tables S7–S12 and Figures S54–S95). For all these molecules the configurations at C3 were deduced from the structure of their precursor **10a** or **10b**, while the relative orientation of the additional stereocentres in compounds **18–22** was determined by NOESY spectroscopy, ultimately allowing for full structure elucidation of all six compounds (for **19** vide *infra*).

During the biosynthesis of **18–22** a similar 1,3-hydride shift as from cation **A** to **B** can be assumed. To investigate this hydride migration, (1,1-²H₂)-**8a** and (1,1-²H₂)-**8b** were synthesised (Scheme S2A, Supporting Information) and enzymatically converted with (7-¹³C)GPP^[19] by FPPS and TmS. ¹³C-NMR analysis of the obtained products established the proposed hydride migrations by slightly upfield shifted triplets for C11, indicating a direct ¹³C–²H bond (Figures S96 and S97). The hydride migrations were further supported by GC-EIMS analysis in which the *iPr* groups of **18–22** are lost by α -cleavage, allowing to locate deuterium within this group (Figures S98 and S99). The specific migration of the enantiotopic C1 hydrogens in FPP in the 1,3-hydride shift from **A** to **B** depends on the configuration at C7 of **A**, with migration of H_S for (*S*)-**A** and of H_R for (*R*)-**A**.^[18] Conclusively, if the stereocentre at C7 is retained in the final prod-

uct, the fate of H_S and H_R can serve as a marker to determine absolute configurations. This strategy was also applied to the methylated sesquiterpene analogues obtained with TmS by synthesis of (*R*)- and (*S*)-(1-¹³C,1-²H)-**8a**, and (*R*)- and (*S*)-(1-¹³C,1-²H)-**8b** (Scheme S2B) that were all obtained in high enantiomeric purity (Figure S100). Their incubation with GPP, FPPS and TmS showed for **18–22** migration of the 1-*pro-S* hydrogen of **10a** or **10b** into the *iPr* group (Figures S101–S105), whereas the 1-*pro-R* hydrogen remains bound to C6 of **18–21**, which further supports their assigned absolute configurations (Figures S101–S104). Only for **22** the deuterium label ends up in a neighbouring position (C1) as indicated by a characteristic $\Delta\delta = -0.07$ ppm for the labelled carbon (Figure S105). For **17** a specific stereochemical course for the C1 hydrogens was observed by product analysis through HSQC spectroscopy, revealing that the 1-*pro-R* hydrogen ends up in the H1_Z and the 1-*pro-S* hydrogen in the H1_E position (Figure S106), which supports its enzymatic formation and reflects the situation in the intermediate (*R*)-NPP towards **16** (Scheme 4 A). For the biosynthesis of **22** another 1,2-hydride shift from C6 to C7 of **10b** was assumed. Direct evidence for this step was obtained by incubation of (3-¹³C,2-²H)GPP and **8b** with FPPS and TmS, resulting in an upfield shifted triplet for C10 of **22** as a result of ¹³C–²H spin coupling (Figure S107). The terminal deprotonation to this compound was followed by incubation of (2-²H)DMAPP,^[20] IPP and **8b** with FPPS and TmS. The main product of this reaction was (7-²H)-**16**, but unlabelled **22** was also detected (Figure S108).

It is well known that the elongation of oligoprenyl diphosphates with IPP proceeds with inversion of configuration at C1 of the allyl diphosphate^[21] and *Si* face attack at C4 of IPP.^[15] As discussed above, the face selectivity regarding the IPP analogues **8a** and **8b** is the same. To investigate whether also configuration inversion at C1 of the allyl diphosphate occurs, (*R*)- and (*S*)-(1-¹³C,1-²H)GPP^[22] and **8a** or **8b** were incubated with FPPS and TmS. HSQC analysis of the obtained products revealed selective deuterium incorporation into H2_β of **18**, **20** and **22** from (*R*)- and into H2_α from (*S*)-(1-¹³C,1-²H)GPP (Figures S109–S111, Supporting Information), in agreement with configurational inversion. Based on these findings, an NMR data assignment for the diastereotopic C5 hydrogens of **17** was possible (Figure S112). Also, the NMR shifts of the C2 hydrogens of **19** could be assigned (Figure S113), which allowed for its unambiguous configuration determination, that was without this information obscured by the identical chemical shifts of H1 and H2_α. Through this labelling strategy also the C2 hydrogens of **21** with almost identical chemical shifts were distinguished (Figure S114, 1.75 ppm for H2_α and 1.72 ppm for H2_β).

In summary, we have demonstrated that methylated IPP analogues can be enzymatically incorporated into methylated terpenes, giving access to a chemical space that is naturally realised only in a few known cases. The incorporation sites of the extra Me groups set a stereochemical anchor in the products that allows to assign their absolute configurations. In conjunction with labelling experiments complex and interesting stereochemical problems and enzyme mechanistic aspects can

be solved. We will extend this work in the future using further IPP analogues and TSs for the enzymatic synthesis of methylated terpenes.

Acknowledgements

This work was funded by the DFG (DI1536/7-1). We thank Andreas Schneider for HPLC purifications.

Conflict of interest

The authors declare no conflict of interest.

Keywords: configuration determination · enzyme catalysis · isotopes · substrate analogues · terpenoids

- [1] J. S. Dickschat, *Angew. Chem. Int. Ed.* **2019**, *58*, 15964; *Angew. Chem.* **2019**, *131*, 16110.
- [2] J. S. Dickschat, *Nat. Prod. Rep.* **2016**, *33*, 87.
- [3] M. B. Quin, C. M. Flynn, C. Schmidt-Dannert, *Nat. Prod. Rep.* **2014**, *31*, 1449.
- [4] A. Minami, T. Ozaki, C. Liu, H. Oikawa, *Nat. Prod. Rep.* **2018**, *35*, 1330.
- [5] T. Mitsunashi, I. Abe, *ChemBioChem* **2018**, *19*, 1106.
- [6] D. W. Christianson, *Chem. Rev.* **2017**, *117*, 11570.
- [7] R. J. Peters, *Nat. Prod. Rep.* **2010**, *27*, 1521.
- [8] a) J. S. Dickschat, T. Nawrath, V. Thiel, B. Kunze, R. Müller, S. Schulz, *Angew. Chem. Int. Ed.* **2007**, *46*, 8287; *Angew. Chem.* **2007**, *119*, 8436; b) M. Komatsu, M. Tsuda, S. Omura, H. Oikawa, H. Ikeda, *Proc. Natl. Acad. Sci. USA* **2008**, *105*, 7422; c) C.-M. Wang, D. E. Cane, *J. Am. Chem. Soc.* **2008**, *130*, 8908.
- [9] a) S. H. von Reuß, M. Kai, B. Piechulla, W. Francke, *Angew. Chem. Int. Ed.* **2010**, *49*, 2009; *Angew. Chem.* **2010**, *122*, 2053; b) S. von Reuß, D. Domicck, M. C. Lemfack, N. Magnus, M. Kai, T. Weise, B. Piechulla, *J. Am. Chem. Soc.* **2018**, *140*, 11855.
- [10] T. Ozaki, S. S. Shinde, L. Gao, R. Okuizumi, C. Liu, Y. Ogasawara, X. Lei, T. Dairi, A. Minami, H. Oikawa, *Angew. Chem. Int. Ed.* **2018**, *57*, 6629; *Angew. Chem.* **2018**, *130*, 6739.
- [11] D. A. Schooley, K. J. Judy, B. J. Bergot, M. S. Hall, J. B. Siddall, *Proc. Natl. Acad. Sci. USA* **1973**, *70*, 2921.
- [12] a) D. J. Miller, F. Yu, R. K. Allemann, *ChemBioChem* **2007**, *8*, 1819; b) J. A. Faraldos, Y. Zhao, P. E. O'Maille, J. P. Noel, R. M. Coates, *ChemBioChem* **2007**, *8*, 1826; c) O. Cascón, S. Touchet, D. J. Miller, V. Gonzalez, J. A. Faraldos, R. K. Allemann, *Chem. Commun.* **2012**, *48*, 9702; d) S. Touchet, K. Chamberlain, C. M. Woodcock, D. J. Miller, M. A. Birkett, J. A. Pickett, R. K. Allemann, *Chem. Commun.* **2015**, *51*, 7550; e) M. Demiray, X. Tang, T. Wirth, J. A. Faraldos, R. K. Allemann, *Angew. Chem. Int. Ed.* **2017**, *56*, 4347; *Angew. Chem.* **2017**, *129*, 4411; f) C. Oberhauser, V. Harms, K. Seidel, B. Schröder, K. Ekramzadeh, S. Beutel, S. Winkler, L. Lauterbach, J. S. Dickschat, A. Kirschning, *Angew. Chem. Int. Ed.* **2018**, *57*, 11802; *Angew. Chem.* **2018**, *130*, 11976.
- [13] P. Rabe, J. Rinkel, B. Nubbemeyer, T. G. Köllner, F. Chen, J. S. Dickschat, *Angew. Chem. Int. Ed.* **2016**, *55*, 15420; *Angew. Chem.* **2016**, *128*, 15646.
- [14] T. Koyama, K. Ogura, S. Seto, *J. Am. Chem. Soc.* **1977**, *99*, 1999.
- [15] J. W. Cornforth, R. H. Cornforth, G. Popjak, L. Yengoyan, *J. Biol. Chem.* **1966**, *241*, 3970.
- [16] a) P. Rabe, J. S. Dickschat, *Angew. Chem. Int. Ed.* **2013**, *52*, 1810; *Angew. Chem.* **2013**, *125*, 1855; b) P. Rabe, T. Schmitz, J. S. Dickschat, *Beilstein J. Org. Chem.* **2016**, *12*, 1839.
- [17] M. Winter, H. Schinz, M. Stoll, *Helv. Chim. Acta* **1947**, *30*, 2213.
- [18] J. Rinkel, P. Rabe, P. Garbeva, J. S. Dickschat, *Angew. Chem. Int. Ed.* **2016**, *55*, 13593; *Angew. Chem.* **2016**, *128*, 13791.
- [19] T. Mitsunashi, J. Rinkel, M. Okada, I. Abe, J. S. Dickschat, *Chem. Eur. J.* **2017**, *23*, 10053.

- [20] J. Rinkel, P. Rabe, X. Chen, T. G. Köllner, F. Chen, J. S. Dickschat, *Chem. Eur. J.* **2017**, *23*, 10501.
- [21] J. W. Cornforth, R. H. Cornforth, C. Donninger, G. Popjak, *Proc. R. Soc. London Ser. B* **1966**, *163*, 492.
- [22] P. Rabe, J. Rinkel, E. Dolja, T. Schmitz, B. Nubbemeyer, T. H. Luu, J. S. Dickschat, *Angew. Chem. Int. Ed.* **2017**, *56*, 2776; *Angew. Chem.* **2017**, *129*, 2820.

Manuscript received: January 2, 2020

Accepted manuscript online: January 3, 2020

Version of record online: January 30, 2020
